

Restoration of retinal morphology and residual scarring after photocoagulation

Daniel Lavinsky,^{1,2} Jose A. Cardillo,¹ Yossi Mandel,²
Philip Huie,² Luiz A. Melo,¹ Michel E. Farah,¹
Rubens Belfort¹ and Daniel Palanker²

¹Department of Ophthalmology, Federal University of Sao Paulo, Sao Paulo, Brazil

²Department of Ophthalmology and Hansen Experimental Physics Laboratory, Stanford University, Stanford, California, USA

ABSTRACT.

Purpose: To study healing of retinal laser lesions in patients undergoing PRP using SD-OCT.

Methods: Moderate, light and barely visible retinal burns were produced in patients with proliferative diabetic retinopathy scheduled for PRP using 100-, 20- and 10-ms pulses of 532-nm laser, with retinal spot sizes of 100, 200 and 400 μm . Lesions were measured with OCT at 1 hr, 1 week, 1, 2, 4, 6, 9 and 12 months. OCT imaging was correlated with histology in a separate study in rabbits.

Results: Lesions produced by the standard 100-ms exposures exhibited steady scarring, with the damage zone stabilized after 2 months. For 400- and 200- μm spots and 100-ms pulses, the residual scar area at 12 months was approximately 50% of the initial lesion size for moderate, light and barely visible burns. In contrast, lesions produced by shorter exposures demonstrated enhanced restoration of the photoreceptor layer, especially in smaller burns. With 20-ms pulses, the damage zone decreased to 32%, 24% and 20% for moderate, light and barely visible burns of 400 μm , respectively, and down to 12% for barely visible burns of 200 μm . In the 100- μm spots, the residual scar area of the moderate 100-ms burns was 41% of the initial lesion, while barely visible 10-ms burns contracted to 6% of the initial size. Histological observations in rabbits were useful for proper interpretation of the damage zone boundaries in OCT.

Conclusions: Traditional photocoagulation parameters (400 μm , 100 ms and moderate burn) result in a stable scar similar in size to the beam diameter. Restoration of the damaged photoreceptor layer in lighter lesions produced by shorter pulses should allow reducing the common side-effects of photocoagulation such as scotomata and scarring.

Key words: laser photocoagulation – optical coherence tomography – plasticity – wound healing

Acta Ophthalmol. 2013; 91: e315–e323

© 2013 The Authors

Acta Ophthalmologica © 2013 Acta Ophthalmologica Scandinavica Foundation

doi: 10.1111/aos.12045

Introduction

The Diabetic Retinopathy Study established panretinal photocoagulation (PRP) as an effective treatment for proliferative diabetic retinopathy (ETDRS, 1991). While the exact mechanism of laser treatment is still debated, one working assumption is that panretinal photocoagulation reduces ischaemia and decreases the production of angiogenic factors in the poorly perfused portions of the retina by killing a fraction of the retinal cells and thus lowering the metabolic load (Jennings et al. 1991; Ishida et al. 1998; Spranger et al. 2000; Sánchez et al. 2007). Photoreceptors are the most numerous and metabolically active cells in the retina with high oxygen consumption. The inner retinal cells (INL and GCL) represent < 10% of the number of photoreceptors (Jonas et al. 1992; Aggarwal et al. 2007), so additional damage to the inner retina is unlikely to significantly improve clinical efficacy. Other theories include improvement of oxygenation and metabolic transport between choroid and retina by creating photoreceptor-free glial ‘windows’ (Stefánsson et al. 1981; Molnar et al. 1985; Pournaras et al. 1990; Stefánsson 2006), and stimulation of RPE and choroidal cells by thermal stress (Mainster & Reichel 2001).

Traditionally, photocoagulation with a 514- or 532-nm laser was produced using pulses of 100–200 ms in

duration and spot sizes ranging from 200–500 μm (ETDRS 1987a,b). Such long-pulse photocoagulation often causes damage not only to photoreceptors but also to the inner retina and even nerve fibre layer (Schatz et al. 1991). Retinal scarring following conventional photocoagulation may enlarge over time, causing additional loss of visual field (Schatz et al. 1991; Maeshima et al. 2004).

Recently, a new method of retinal photocoagulation has been introduced, in which patterns of spots are applied with a single press of a foot pedal using a scanning laser with pulse durations in the range of 10–30 ms (PASCAL; Topcon, USA) (Blumenkranz et al. 2006). As heat diffusion with shorter exposures is decreased, these lesions tend to be lighter and smaller than conventional burns and have better localization of the damage to the outer retina (Jain et al. 2008; Paulus et al. 2008; Nagpal et al. 2010; Palanker et al. 2011). As lighter lesions tend to be smaller (Jain et al. 2008), a larger number of such spots should be applied to coagulate the same total area of the retina during PRP (Palanker et al. 2011).

Studies of retinal healing after photocoagulation in animals demonstrated remarkable shift of photoreceptors from adjacent untreated areas into the coagulated zone, restoring continuity of the photoreceptor layer in lighter and smaller lesions (Paulus et al. 2008; Belokopytov et al. 2010). Spectral domain optical coherence tomography (SD-OCT) has been applied to follow up retinal lesions in patients. However, these studies were limited to larger retinal spot sizes (300–400 μm) and only 6-month follow-up (Kriechbaum et al. 2010; Muqit et al. 2011).

This study describes the acute morphology of retinal photocoagulation lesions and their healing over a 12-month follow-up period. It explores the whole range of clinically relevant spot sizes, pulse durations and clinical grades. SD-OCT is initially correlated with histology in animal models and then applied to patients undergoing PRP. The study demonstrates restoration of retinal anatomy over time in smaller and lighter lesions, which may allow minimizing or even completely avoiding the current detrimental side-effects of retinal laser therapy – scotomata and scarring.

Methods

OCT-histology correlation study

Two pigmented Dutch Belted rabbits (1.5–2.5 kg) were used in accordance with the ARVO Statement Regarding the Use of Animals in Ophthalmic and Vision Research after approval from the Stanford University Animal IRB. The rabbits were anesthetized using ketamine hydrochloride (35 mg/kg), xylazine (5 mg/kg) and glycopyrrolate (0.01 mg/kg) administered intramuscularly 15 min before the procedure. Pupillary dilation was achieved by one drop each of 1% tropicamide and 2.5% phenylephrine hydrochloride. One drop of topical tetracaine at 0.5% was instilled in each eye before treatment.

Laser photocoagulation was conducted using PASCAL Streamline laser (Topcon Medical Laser Systems, Santa Clara, CA, USA) and a Mainster wide field retinal laser contact lens (Ocular Instruments, Bellevue, WA, USA), which provides retinal beam size equal to the aerial in a rabbit eye. Power and duration were titrated to produce intense, moderate, light and barely visible burns with 400- μm beam. Retinal lesions were imaged at 1 hr, 1 week, 1 and 2 months with SD-OCT (Spectralis; Heidelberg Engineering, Heidelberg, Germany). After 2 months, eyes were enucleated and fixed for light microscopy (LM). Direct correlation between OCT and histology was performed at various time-points to determine the interpretation of various tissue layers, the edges of the damage zone and boundaries of the glial plug in the lesion. Armed with this knowledge, we could then quantify the retinal lesions measured with OCT in human patients over time. In particular, we evaluated the width of damage zone at the RPE–photoreceptors junction, the presence of the inner/outer segments junction line and abnormalities in the inner retina.

Patient selection and clinical study design

A prospective, interventional, open-label trial was conducted with proliferative diabetic retinopathy patients scheduled for PRP. The study was conducted according to tenets of the Declaration of Helsinki with approval

from the Federal University of Sao Paulo Ethics and Research Committee and was registered at clinicaltrials.gov (NCT01304225). All patients gave their informed consent. OCT was performed immediately after photocoagulation, 1 week, 1, 2, 4, 6, 9 and 12 months after treatment. PRP was completed after 1 month of the initial treatment.

Treatment procedures

Photocoagulation was performed using PASCAL laser (532-nm wavelength). With the area centralis contact lens (magnification $\times 0.94$; Volk, Mentor, OH, USA), aerial beam diameters of 100, 200 and 400 μm corresponded to retinal beam diameters of 94, 188 and 376 μm , respectively. Lesions of ‘moderate’ clinical grade were produced with 100-ms pulses using 100-, 200- and 400- μm beam. As the laser power could not be decreased below 100 mW, the ‘light’ and ‘barely visible’ lesions could only be produced with 100-ms exposures using the 400- μm spot, but not with 200 and 100 μm . With 20-ms pulses, all three clinical grades – ‘moderate’, ‘light’ and ‘barely visible’ – were produced with all 3 beam sizes. Laser power for each pulse duration was first titrated peripheral to retinal arcades to create a moderate (white-grey) lesion, and then, the same power was used to create two moderate lesions temporal to the macula over 3500 μm away from the fovea. For light and barely visible burns, power was reduced by 25% and 50%, respectively, from the moderate 20-ms lesions. Owing to the 100-mW limitation on the minimum laser power, the 100- μm barely visible burn was produced using 10-ms pulse duration.

Measurement of lesion size with OCT

The SD-OCT was used to measure the width of the acute coagulated zone within 1 hr of the procedure. The largest width of the damage zone at the RPE–photoreceptor junction was measured by a single examiner using the caliper provided by the Heidelberg Eye Explorer software (Heidelberg Engineering). In addition, the borders of the hyper-reflective lesion at the RPE–photoreceptor junction, position of external (outer) limiting membrane (ELM) and the line of the inner/outer

photoreceptors segments junction were noted. Scan averaging was applied to reduce speckle noise and improve resolution and identification of intraretinal details. The use of an image tracking system (TruTracktm; Heidelberg Engineering) enabled measurement of the same retinal area on each follow-up visit, ensuring proper assessment of progressive changes of the lesion size during the study. The axial resolution of 7 μm and transverse resolution of 14 μm rendered the acquisition of high-quality images that allowed the study of the retinal and laser burn morphology in detail (Kriechbaum et al. 2010).

Statistical analysis

Data are reported as mean \pm standard deviation (SD) for laser beam diameter, the ratio of the lesion to beam size and the residual lesion area. The statistical analysis was performed using the statistical packages Stata12.0 (StatCorp, College Station, TX, USA) and Statistica 8.0 (Statsoft, Inc., Tulsa, OK, USA). The Friedman's analysis of variance was used to evaluate the changes in the lesion size within each treatment group throughout the study. The lesion size at each follow-up visit was compared between groups using the Kruskal–Wallis test. Owing to multiple comparisons, the significance level was set at 0.01 rather than 0.05.

Results

OCT-histology correlation study

Two pigmented (Dutch Belted) rabbits were included in this experiment, and a total of 200 lesions were analysed with OCT and histologically with light microscopy (LM). Intense and moderate burns appeared clinically with a white centre and grey rim. Light burns had a smaller, central, white burn with larger grey rim. The barely visible lesions only had grey discoloration of the retina.

Intense and moderate burns induced acute damage to the whole retina thickness with disruption of the nerve fibre layer and bulging of the inner retina on OCT and LM (Fig. 1A,B). Disruption of the inner and outer nuclear layers seen on histology appeared on OCT as increased reflectivity bands.

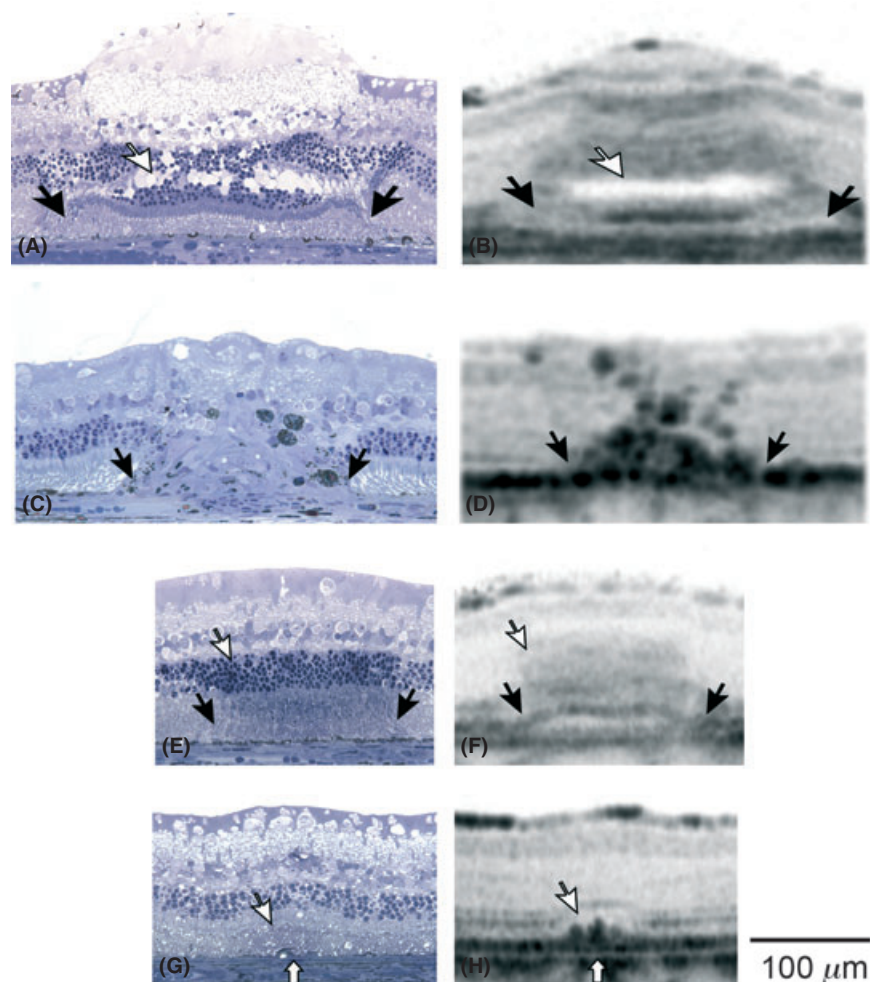


Fig. 1. Light microscopy and OCT of intense and barely visible 400- μm laser burn in rabbit retina. (A) Acute intense burn exhibiting damage to outer segments and photoreceptor nuclei, vacuolization (white arrow), separation of IS/OS layer and ONL, disruption of OPL, INL and IPL, as well as marked oedema of the nerve fibre layer. Edge of the damage zone can be identified as intense oblique line in photoreceptors layer as well pyknotic nuclei in the ONL (black arrow). (B) OCT of acute intense burn with a hyper-reflective line in the outer segments area (black arrows) and hyporeflexive zone of vacuolization (white arrow), disruption of normal outer and inner retina architecture and oedema. (C and D) LM and OCT appearance of intense burn at 2 months exhibiting total loss of photoreceptors and presence of glial plug in the centre of the burn (black arrows). (E and F) Acute LM and OCT features of barely visible burn with localized effect in the outer retina and well-defined borders of the damage zone having mild coagulation of the inner/outer segments and pyknotic photoreceptors nuclei (white arrow) correlating with a hyper-reflective vertical band on OCT (black arrows). (G and H) After 2 months, there is a complete restoration of photoreceptors layer. IS/OS junction line can be clearly seen in OCT (white arrow), and RPE hypertrophy and irregularity is identified on both LM and OCT (vertical white arrow).

Vacuolization and separation of the outer nuclear layer from photoreceptors corresponded to a low reflectivity space on OCT. Damage to the photoreceptor segments in the centre of the intense and moderate burns appeared as a highly reflective band above RPE. The demarcation line between the damaged and normal photoreceptors seen in LM appeared as a hyper-reflective oblique band on OCT (Fig. 1A,B). This feature was used for the measurement of the lesion width in the follow-

ing human studies. After 2 months, there was a significant central gliotic scar, which appeared hyper-reflective on OCT. Glial origin of the retinal scar tissue was previously demonstrated by immunohistochemical analysis demonstrating GFAP (glial fibrillary acidic protein) expression between 3 days and 4 months (Leung et al. 2010). The lack of photoreceptors in this area could be identified by the absence of the inner/outer segment layer on OCT (Fig. 1C,D).

Light and barely visible burns affected mainly the RPE and photoreceptor layers, including the outer nuclear layer (ONL). A distinct area with increased reflectivity was clearly visible in OCT, corresponding to damaged photoreceptors: their inner/outer segments and pyknotic nuclei (Fig. 1E,F). In 2 months, a complete resolution of damage in photoreceptor layer of the barely visible lesions was observed, including restoration of ELM and IS/OS layer, as identified by OCT. However, a hyper-reflective irregularity in the RPE layer could still be observed, which correlated with hypertrophic RPE changes on LM (Fig. 1G,H).

Clinical study

Thirty eyes of 22 patients with PDR were included, and a total of 520 lesions were measured with SD-OCT. Seventy-two per cent of all patients were white, 9% black and 19% mixed; 73% were men and 27% were women. Mean age was 54 years (range 19–70). Average laser powers (mW) for different photocoagulation clinical end-points, pulse duration and spot sizes are summarized in Table 1. Lesions of the light and barely visible clinical grades were not applied with 100-ms pulses using 200- and 100- μ m spot sizes because the minimum laser power (100 mW) was too high. After the correlation experiment in rabbits, the retinal layers and laser burn boundaries were defined on OCT as shown in Fig. 2, and the damage zone width was measured according to these features.

400- μ m spot size

A total of 240 laser lesions were applied with 400- μ m spot size, 40 for each clinical end-point and pulse duration (moderate, light and barely visible with 100- and 20-ms pulses). Changes in the retinal reflectivity

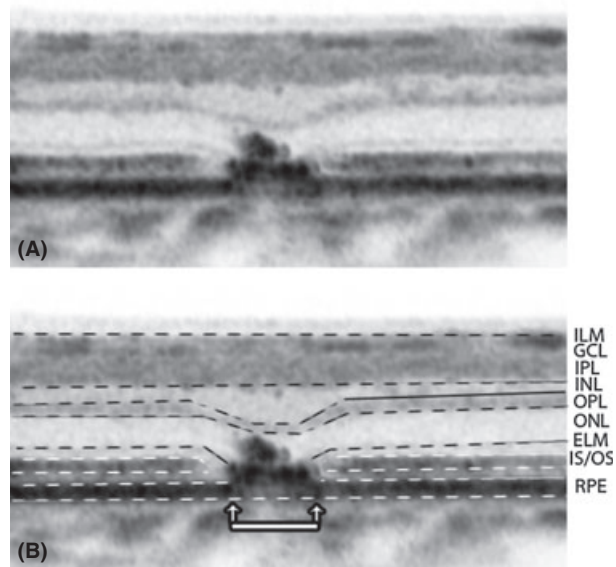


Fig. 2. (A) OCT of a laser lesion in human retina 3 months after photocoagulation. (B) Retinal layers are outlined with dark and white dashed lines. Laser damage zone at the RPE–photoreceptor junction is indicated by two arrows connected with a white line. ILM, internal limiting membrane; GCL, ganglion cell layer; IPL, inner plexiform layer; INL, inner nuclear layer; OPL, outer plexiform layer; ONL, outer nuclear layer; ELM, external limiting membrane; IS/OS, inner/outer segments junction line; RPE, retinal pigment epithelium.

immediately following the moderate 100-ms exposures included increased reflectivity in the RPE, outer and inner retina layers (Fig. 3B). Retinal thickness increased at the burn site, a hyper-reflective band could be seen at the ganglion cell layer (GCL) and nerve fibre layer (NFL), a hyporeflexive area appeared at the outer nuclear layer (ONL), and the inner/outer (IS/OS) photoreceptor segments junction line disappeared. Light 100-ms burns also presented a hyper-reflective band in the RPE and photoreceptors, but there was less retinal thickening, reduced hyper-reflectivity in the nerve fibre layer and no hyporeflexive area in the outer nuclear layer. Changes in the barely visible 100-ms burns were limited to hyper-reflectivity in RPE and photoreceptors. Mean lesion diameters with 100-ms exposures were 538 \pm 35, 446 \pm 50 and 370 \pm 36 μ m for moderate, light and barely vis-

ible lesions, respectively ($p < 0.001$) (Fig. 4).

For all clinical grades, the lesions produced with 20-ms pulses were smaller than with 100 ms and had less inner retinal damage. RPE and photoreceptors still exhibited increased reflectivity. Moderate burns had slightly enhanced reflectivity in the GCL. Changes in the light and barely visible 20-ms lesions were limited to focal detachment of the RPE and enhanced reflectivity of the photoreceptor layer, while the inner retina was perfectly preserved (Fig. 3H,K). Mean lesion diameters were 430 \pm 33, 367 \pm 35 and 279 \pm 44 μ m for moderate, light and barely visible lesions, respectively ($p < 0.001$) (Fig. 4).

Subsequent measurements at 1 week, 1, 2, 4, 6, 9 and 12 months demonstrated a continuous process of contraction and stabilization of a scar (Figs 4 and 5). The 100-ms lesions

Table 1. Mean laser power (mW) for different photocoagulation clinical end-points, pulse duration and spot sizes.

	Moderate 100 ms	Light 100 ms	Barely visible 100 ms	Moderate 20 ms	Light 20 ms	Barely visible 20 ms	Barely visible 10 ms
100 μ m	160 \pm 24	–	–	215 \pm 45	150 \pm 26	–	112 \pm 17
200 μ m	175 \pm 47	–	–	268 \pm 57	183 \pm 40	133 \pm 26	–
400 μ m	277 \pm 53	220 \pm 74	167 \pm 42	467 \pm 86	372 \pm 59	260 \pm 41	–

Data are shown as mean (mW) \pm SD.

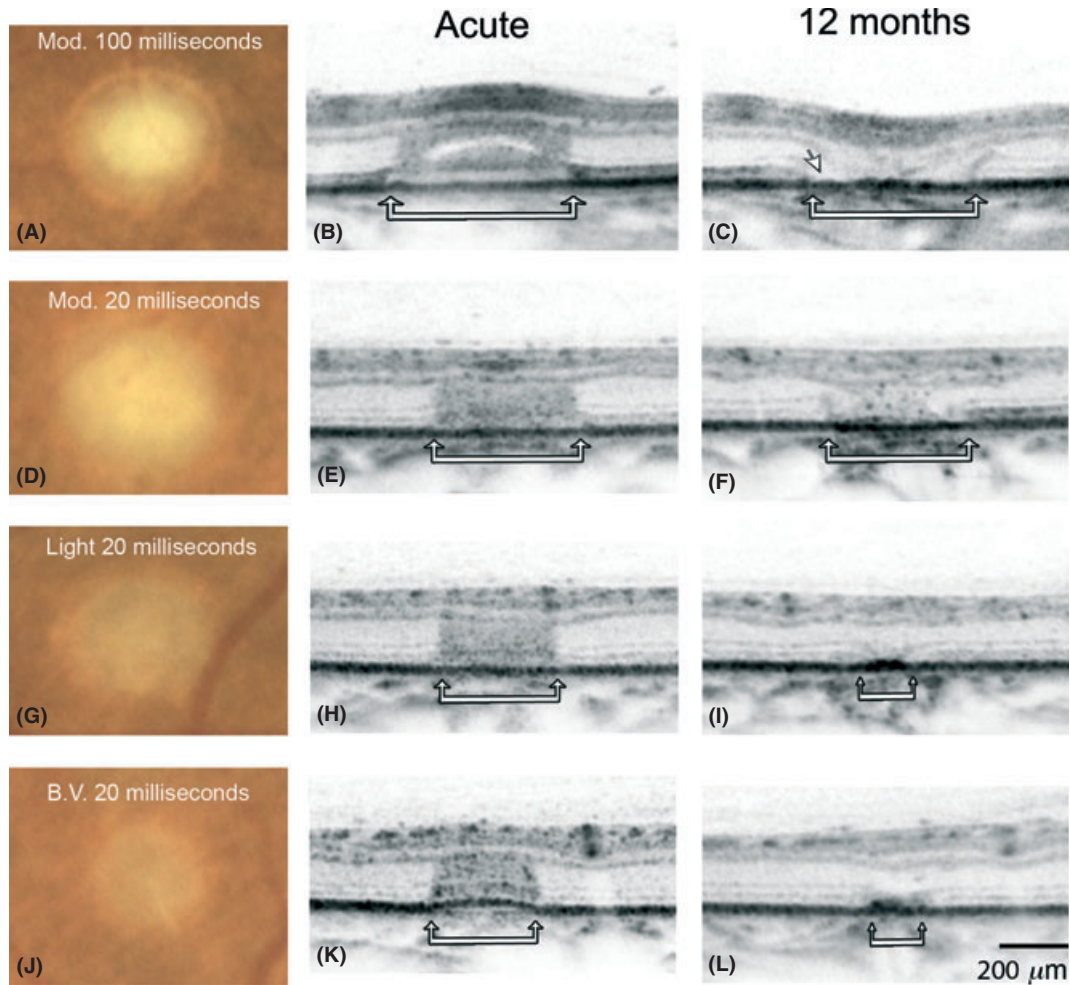


Fig. 3. Acute and 12-month 400- μm laser burns. First row shows acute clinical (A) and OCT (B) appearance of a moderate 100-ms burn, and 12-month follow-up (C). White arrows indicate the scarring area absent of the IS/OS layer. Second row shows acute a moderate 20-ms burn (D–F). Third and fourth (G–L) rows show acute and 12-month results of light and barely visible 20-ms burns, which demonstrates initial damage (hyper-reflectivity) limited to only outer retina, and significant restoration of the outer retina at 12 months.

decreased only during the first 2 months, while the 20-ms lesions continued to contract, as plotted in Fig. 4. Moderate 100-ms lesions showed the greatest residual damage at 12 months, with peripheral defect of surrounding IS/OS layer and traction to the external limiting membrane, with an overall decrease in the retinal thickness, disruption of normal nerve fibre layer, ganglion cell inner nuclear and outer plexiform layer (Fig. 3C). The outer nuclear layer, external limiting membrane and IS/OS junction line were absent in the lesion, and RPE was highly irregular in its centre. The moderate, light and barely visible 100-ms lesions contracted to 52%, 50% and 48% of the original area, respectively ($p < 0.001$) (Fig. 4). The lesion/beam ratio of 100-ms exposures at 12 months was 1.0, 0.85 and 0.66, corresponding to

the final lesion diameters of 383 ± 11 , 319 ± 43 and $250 \pm 20 \mu\text{m}$, respectively. Lesion/beam ratios for all lesions throughout the follow-up period are shown in Table 2.

As shown in Fig. 5 for a light 400- μm , 20-ms burn, the hyperpigmented zone in the outer retina decreased in width during the healing process. At 1 week, the INL shifted down in the lesion, but over time was elevated back towards its normal position. A progressive contraction of the hyper-reflective area in the outer retina could be seen, with some restoration of the IS/OS line at the periphery of the damaged zone. Hyper-reflective area remained in the large central part of the lesion.

At 12 months, the damage zone in photoreceptor layer in the moderate, light and barely visible 20-ms lesions contracted to 32%, 24% and 20% of

the initial lesion area, respectively ($p < 0.001$) (Fig. 4). The lesion/beam ratio at 12 months for 20-ms exposures was 0.63, 0.46 and 0.29, and final lesion diameters of 240 ± 24 , 176 ± 26 and $112 \pm 28 \mu\text{m}$ for moderate, light and barely visible grades, respectively.

200- μm spot size

A total of 140 laser lesions were applied with 200- μm spot size, 20 for 100-ms moderate grade and 40 for moderate, light and barely visible 20-ms exposures. Similar morphologic characteristics as with 400- μm spot size were detected immediately after the laser treatment (Fig. 6). With 20-ms exposures, all the clinical grades presented changes in reflectivity limited to the photoreceptor layer. As shown in Fig. 4, acute lesion diame-

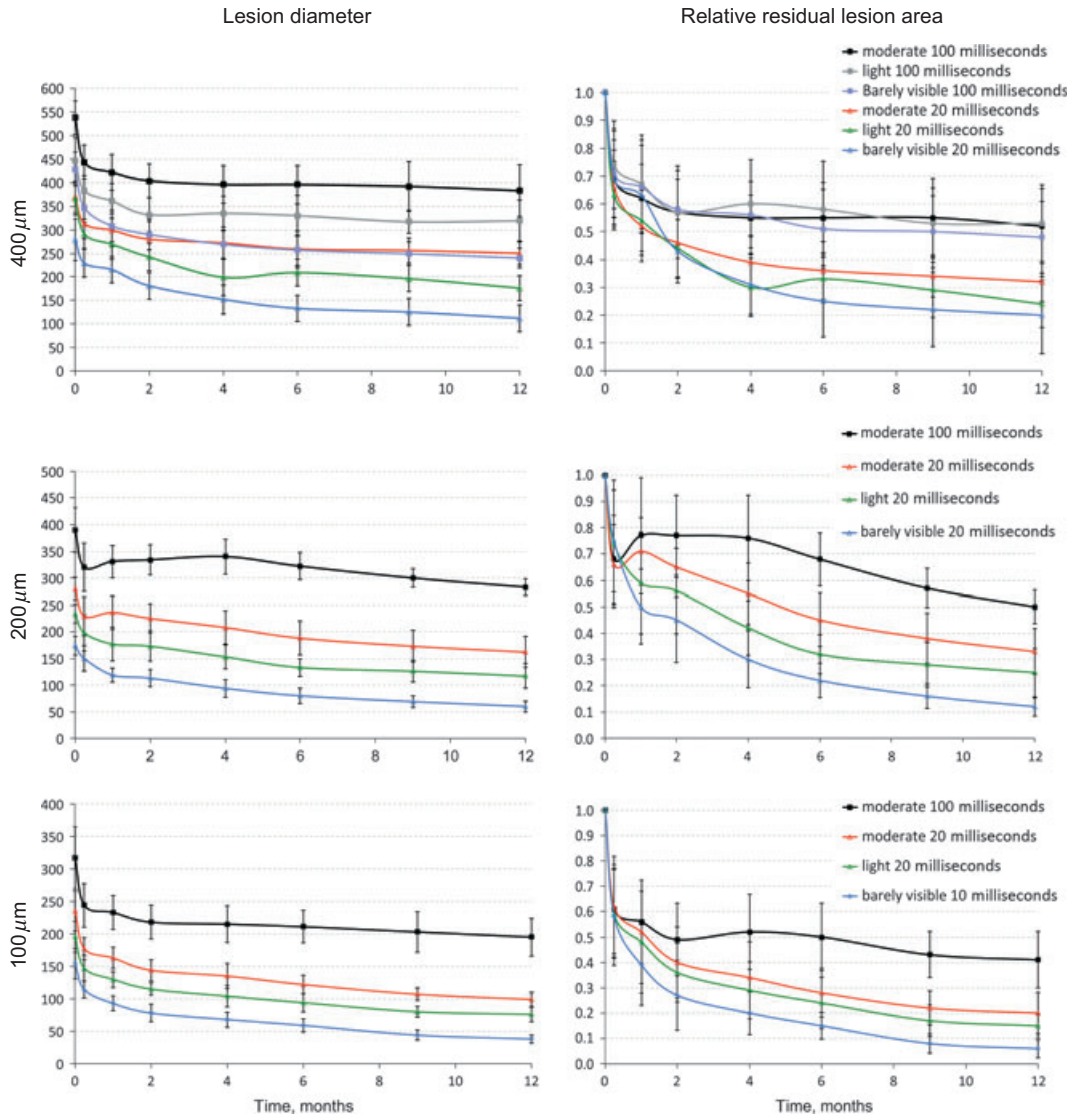


Fig. 4. Lesion diameter and the residual lesion area relative to its initial size for 400-, 200- and 100-μm laser burns produced by 100-, 20- and 10-ms exposures, plotted as a function of time. Data are shown as mean and standard deviation.

Table 2. Lesion/beam ratio for different photocoagulation clinical end-points, pulse duration, spot sizes and healing time.

Follow-up, months	400 μm						200 μm				100 μm			
	Mod 100 ms	Light 100 ms	Bv 100 ms	Mod 20 ms	Light 20 ms	Bv 20 ms	Mod 100 ms	Mod 20 ms	Light 20 ms	Bv 20 ms	Mod 100 ms	Mod 20 ms	Light 20 ms	Bv 10 ms
0	1.43	1.18	0.98	1.14	0.97	0.74	2.07	1.49	1.24	0.92	3.37	2.50	2.07	1.64
0.25	1.18	1.02	0.83	0.92	0.77	0.60	1.70	1.21	1.05	0.79	2.59	1.88	1.57	1.21
1	1.12	0.96	0.79	0.81	0.71	0.57	1.76	1.26	0.94	0.63	2.48	1.74	1.39	0.99
2	1.07	0.88	0.74	0.77	0.64	0.48	1.77	1.20	0.92	0.60	2.32	1.53	1.22	0.83
4	1.05	0.89	0.72	0.71	0.52	0.40	1.80	1.11	0.81	0.50	2.29	1.43	1.10	0.73
6	1.05	0.87	0.68	0.68	0.55	0.35	1.71	1.00	0.70	0.42	2.25	1.43	1.10	0.73
9	1.04	0.84	0.68	0.66	0.52	0.33	1.59	0.92	0.67	0.36	2.15	1.14	0.85	0.47
12	1.01	0.83	0.66	0.63	0.46	0.29	1.50	0.86	0.62	0.32	2.07	1.06	0.81	0.40

Mod = moderate; BV = barely visible. Data are shown as mean.

ters were 390 ± 41 , 280 ± 20 , 234 ± 17 and $174 \pm 17 \mu\text{m}$, corresponding to the lesion/beam ratio of 2.07, 1.49, 1.24 and 0.92 for moderate 100 and 20 ms, light and barely visible 20 ms, respectively ($p < 0.001$).

After 1 week, there was a significant decrease in lesion size for all end-points and pulse durations. All lesions continued to decrease in size during the 12-month follow-up period, as shown in Table 2 and in Fig. 4. Final

lesion diameters at 12 months were 283 ± 15 , 162 ± 28 , 117 ± 23 and $60 \pm 10 \mu\text{m}$. The relative residual area at 12 months, compared with the initial lesion size, was 50% for the moderate 100 ms, and 33%, 25% and

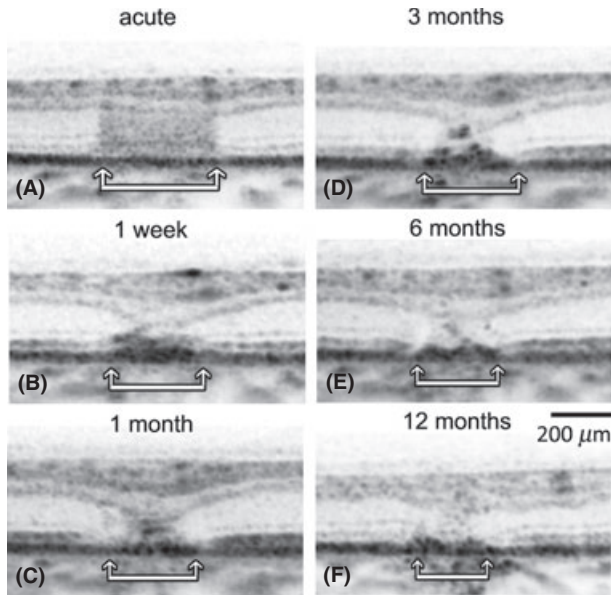


Fig. 5. OCT of light 20-ms 400-µm laser burn at various time-points: acute (A), 1 week (B), 1 month (C), 3 month (D), 6 months (E) and 12 months (F). Two white arrows connected by a line show the width of the damage zone at the photoreceptor/RPE junction. Note progressive restoration of retinal layers architecture over time with limited disruption of the inner retina at 12 months and significant contraction of the damage zone with partial restoration of ELM and IS/OS junction line.

12% for the moderate, light and barely visible 20 ms, respectively ($p < 0.001$). At 12 months, the barely visible burns demonstrated restoration of the external limiting membrane and almost normal appearance of the outer nuclear and plexiform layers, with localized hyper-reflectivity only to RPE and IS/OS junction (Fig. 6l).

100-µm spot size

A total of 140 laser lesions were applied with 100-µm spot size: 20 for moderate 100 ms, 40 for moderate and light 20 ms, and 40 for barely visible 10 ms. The 10-ms pulses were applied to create barely visible burns because the 100 mW low limit of laser power in PASCAL was too high for 20-ms pulses. As shown in Fig. 7, all the 100-µm lesions exhibited changes limited to RPE, photoreceptor segments and ONL. Acute lesion diameters were 317 ± 47 , 235 ± 30 , 195 ± 23 and 154 ± 23 -µm for moderate 100-ms, moderate and light 20-ms, and barely visible 10-ms exposures, respectively ($p < 0.001$) (Fig. 4).

All lesions contracted over time, with the final diameters at 12 months reaching 195 ± 29 , 99 ± 11 , 76 ± 11 and 38 ± 6 µm, corresponding to the lesion/beam ratio of 2.1, 1.1, 0.81 and 0.40, respectively. The residual area of these lesions at 12 months was 41%, 20%, 15% and 6% of the initial lesions, respectively ($p < 0.001$) (Fig. 4 and Table 2).

Discussion

The present study provides a comprehensive assessment of long-term changes in retinal photocoagulation lesions produced with various spot sizes, pulse durations and clinical grades in patients, using high-resolution OCT. Although SD-OCT is widely used in clinical practice as a reliable tool for measurement of retinal anatomical characteristics and pathology, identification of the lesion boundaries is not yet standardized. Therefore, we conducted an animal correlation study to properly relate the optical characteristics of the tissue to actual morphological changes observed with histologically in laser lesions.

Restoration of RPE continuity within days after photocoagulation

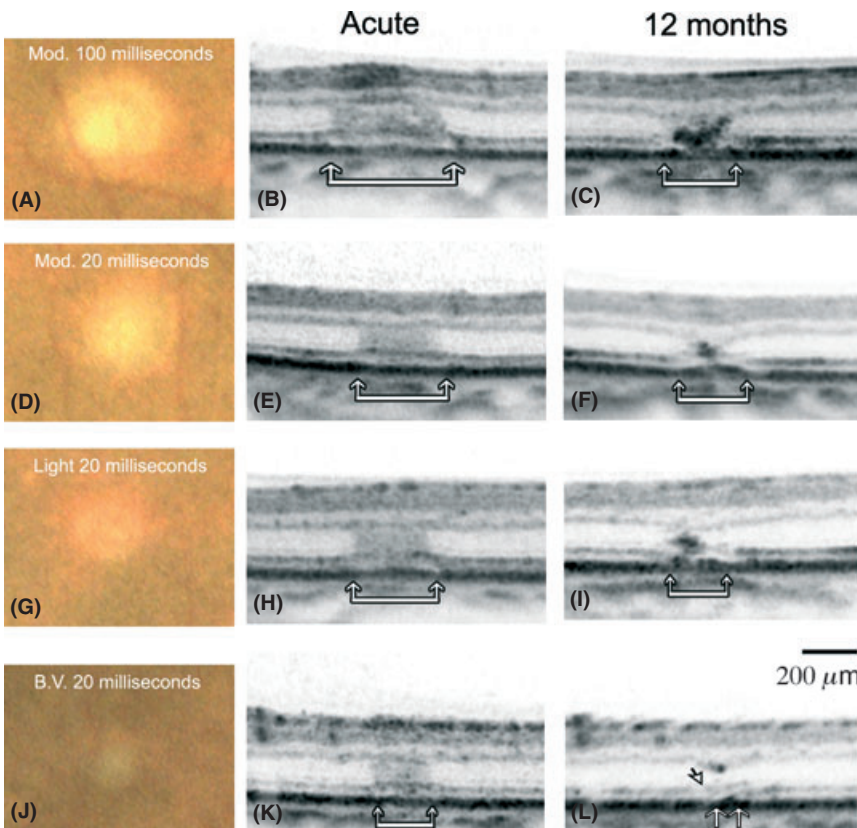


Fig. 6. Two hundred micrometer laser burns. First row shows acute clinical (A) and OCT (B) appearance of a moderate 100-ms burn and its 12-month follow-up (C). Second row shows acute clinical and OCT images (D and E) of a moderate 20-ms burn and its 12-month appearance (F). Note partial restoration of ELM. Third and fourth (G–L) rows show barely visible 20-ms burn, with acute damage limited to outer retina. Note a significant healing of photoreceptors layer (white arrow – IS/OS junction line), more significantly for barely visible burn at 12 months.

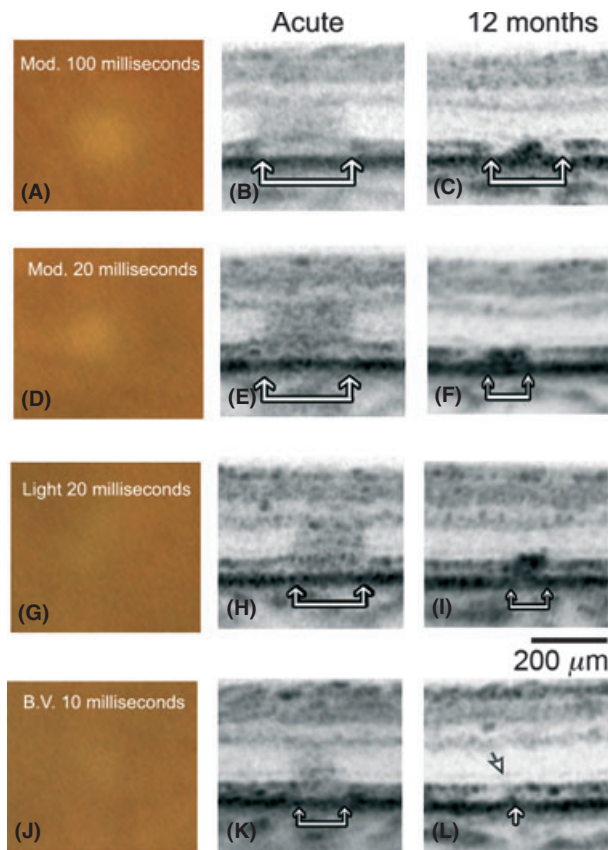


Fig. 7. One hundred micrometer laser burns. First row shows acute clinical (A) and OCT (B) appearance of a moderate 100-ms burn and its 12-month follow-up (C). Retinal damage is limited to the photoreceptors layer and RPE in all laser lesions. Second and third rows show acute clinical (D, G), acute and 12-month OCT (E–I) images of the moderate and light 20-ms lesions. Fourth row shows acute (J–K) and 12-month (L) results with a barely visible 10-ms burn, demonstrating the most significant healing of IS/OS junction line (white arrow), with some residual RPE irregularities (vertical white arrow).

was demonstrated in rabbits by resolution of fluorescein hyperfluorescence over the laser spots and histologically (Wallow 1984; Paulus et al. 2008), while in human patients, it was confirmed using OCT and angiography (Muqit et al. 2011).

Studies of retinal healing after photocoagulation in rabbits (Paulus et al. 2008) and rats (Belokopytov et al. 2010) demonstrated contraction of the damage zone in photoreceptors layer in lesions of all clinical grades. Barely visible and subvisible burns produced with 200- μm spot sizes exhibited complete restoration of the photoreceptors layer, thereby avoiding permanent scarring observed in more intense and larger lesions (Paulus et al. 2008). In these lesions, glial plug appeared in the coagulated zone within a week, similar to the more intense lesions, but completely withdrew at 4 months. Partial retinal repair after photocoagulation was also observed in cynomolgus monkeys (Wallow 1984). Using multi-

electrode array recordings (Sher et al. 2010) and molecular markers of neural activity (Jones et al. 2011) in rabbits, it has been shown that photoreceptors shifting from the adjacent areas re-establish synapses to neurons in the inner nuclear layer, thereby restoring light sensitivity and local activation of the bipolar and ganglion cells in the former lesion. As there is no evidence of photoreceptor proliferation, rather just a shift from the adjacent untreated areas, the therapeutic goal of PRP – reduction in the number of photoreceptors – is still achieved, but the detrimental side-effects of scotomata and scarring can be avoided. Clinical tests of such ‘minimally damaging’ or ‘restorative’ approach to PRP could use an indirect measure of the effectiveness of PRP in improving retinal oxygenation – the reduction in the retinal blood vessels diameter (Mendri- nos et al. 2010).

Recent clinical studies demonstrated significant reduction in the width of

retinal lesions produced by 20-ms pulses, compared with conventional 100- and 200-ms burns (Kriechbaum et al. 2010; Muqit et al. 2011). However, these studies used only large retinal beam sizes (300–396 μm) and had followed the lesions for only 6 months, hence neither reported a near-complete restoration of the IS/OS junction line and ELM, as we observed in smaller lesions (200 and 100 μm) at 12 months. Current study demonstrates that lighter burns produced by shorter pulses and with smaller spot sizes can heal much more completely than the conventional larger and more aggressive coagulation lesions. Up to 94% of the initial damage zone can recover within 12 months in barely visible 100- μm lesions.

Laser scar creeping with enlargement of the atrophic area is a feared complication of conventional photocoagulation (Schatz et al. 1991; Maeshima et al. 2004), which can lead to progressive loss of visual field, peripheral and night vision, and RPE atrophy. Minimally damaging photocoagulation avoiding the inner retinal damage and allowing restoration of the photoreceptors layer can protect the retina from these common detrimental size effects. It is important to keep in mind though that a larger number of spots should be applied to treat the same total area (Palanker et al. 2011).

Patients treated with ‘modified ETDRS’ protocol demonstrated a continuous improvement in central macular thickness and visual acuity over 12 months, suggesting progressive and cumulative laser effect throughout the follow-up period (Lavinsky et al. 2011). This relatively slow effect of laser photocoagulation has also been demonstrated by the DRCR.net clinical trial comparing mETDRS photocoagulation to intravitreal injections of triamcinolone and more recently to anti-angiogenic pharmacotherapy (DRCR.net et al. 2009; Elman et al. 2011). Slow response to laser therapy could be related, although not limited, to the slow healing process observed in our study, where even after 12 months, laser lesions continued to decrease in width and re-establish the normal outer retina morphology.

In some clinical situations, such as retinal tear blockage, the highly restorative photocoagulation might be detrimental. In these cases, a long-term

chorioadhesion is necessary to effectively protect against retinal detachment. The 400- μm , 100-ms moderate lesion had stable size at 12 months (a lesion/beam ratio of 1.0), with sufficient scarring to cause a long-lasting adhesion of the neurosensory retina to the RPE. However, the 20-ms moderate burn exhibited more restoration, contracting to 32% of the initial area at 12 months, and lighter lesions contracted even further. Therefore, the highly restorative protocols should be used with caution in prophylaxis of retinal detachment, and clinical studies comparing the short and long pulses in this application are necessary.

In summary, we have described the morphological characteristics and progressive decrease in size of retinal photocoagulation lesions across a wide spectrum of clinical grades, pulse durations and spot sizes. These observations suggest that retinal healing occurs with most parameters used in clinical practice, although more significantly with shorter pulse durations, smaller spot sizes and less intense clinical end-points. Traditional photocoagulation parameters (400 μm , 100 ms and moderate burn) result in a stable scar similar in size to the beam diameter. Restoration of the damaged photoreceptor layer in lighter lesions by filling-in from the adjacent untreated areas should allow avoiding the common side-effects of photocoagulation such as scotomata and scarring. As lighter lesions tend to be smaller (Jain et al. 2008), a larger number of such spots should be applied to coagulate the same total area during PRP (Palanker et al. 2011). Clinical trials are needed to compare the therapeutic effects of this highly restorative approach and the conventional protocols in applications to panretinal photocoagulation and macular laser therapy.

Acknowledgements

Manuscript was partially presented at ARVO meeting 2011, Fort Lauderdale, Florida, USA. D. Palanker holds a Stanford University patent on patterned scanning laser photocoagulation licensed to Topcon Medical Laser Systems, with associated equity and royalty interest. D. Lavinsky received the 2012 Guillingham Pan-American fellowship (Pan-American Ophthalmological Foundation and Retina Research Foundation). We would like to thank Roopa Dalal for histological preparations.

References

- Aggarwal P, Nag TC & Wadhwa S (2007): Age-related decrease in rod bipolar cell density of the human retina: an immunohistochemical study. *J Biosci* **32**: 293–298.
- Belokopytov M, Belkin M, Dubinsky G et al. (2010): Development and recovery of laser-induced retinal lesion in rats. *Retina* **30**: 662–670.
- Blumenkranz MS, Yellachich D, Andersen DE et al. (2006): Semiautomated patterned scanning laser for retinal photocoagulation. *Retina* **26**: 370–376.
- Diabetic Retinopathy Clinical Research Network (DRCR.net), Beck RW, Edwards AR et al. (2009): Three-year follow-up of a randomized trial comparing focal/grid photocoagulation and intravitreal triamcinolone for diabetic macular edema. *Arch Ophthalmol* **127**: 245–251.
- Diabetic Retinopathy Clinical Research Network, Elman MJ, Bressler NM et al. (2011): Expanded 2-year follow-up of ranibizumab plus prompt or deferred laser or triamcinolone plus prompt laser for diabetic macular edema. *Ophthalmology* **118**: 609–614.
- Early Treatment Diabetic Retinopathy Study Research Group (1987a): Techniques for scatter and local photocoagulation treatment of diabetic retinopathy: Early Treatment Diabetic Retinopathy Study Report no. 3. *Int Ophthalmol Clin* **27**: 254–264.
- Early Treatment Diabetic Retinopathy Study Research Group (1987b): Treatment techniques and clinical guidelines for photocoagulation of diabetic macular edema. Early Treatment Diabetic Retinopathy Study Report Number 2. *Ophthalmology* **94**: 761–774.
- Early Treatment Diabetic Retinopathy Study Research Group (1991): Early photocoagulation for diabetic retinopathy. ETDRS report number 9. *Ophthalmology* **98**: 766–785.
- Ishida K, Yoshimura N, Yoshida M et al. (1998): Upregulation of transforming growth factor-beta after panretinal photocoagulation. *Invest Ophthalmol Vis Sci* **39**: 801–807.
- Jain A, Blumenkranz MS, Paulus Y et al. (2008): Effect of pulse duration on size and character of the lesion in retinal photocoagulation. *Arch Ophthalmol* **126**: 78–85.
- Jennings PE, MacEwen CJ, Fallon TJ et al. (1991): Oxidative effects of laser photocoagulation. *Free Radic Biol Med* **11**: 327–330.
- Jonas JB, Schneider U & Naumann GO (1992): Count and density of human retinal photoreceptors. *Graefes Arch Clin Exp Ophthalmol* **230**: 505–510.
- Jones BW, Huei P & Wang H et al. (2011) Neural activity in the inner retina after photocoagulation. *Invest Ophthalmol Vis Sci* **52**: ARVO e-abstract 5704.
- Kriechbaum K, Bolz M, Deak GG et al. (2010): High-resolution imaging of the human retina *in vivo* after scatter photocoagulation treatment using a semiautomated laser system. *Ophthalmology* **117**: 545–551.
- Lavinsky D, Cardillo JA, Melo LAS et al. (2011): Randomized clinical trial evaluating mETDRS versus normal or high-density micropulse photocoagulation for diabetic macular edema. *Invest Ophthalmol Vis Sci* **52**: 4314–4323.
- Leung L, Leng T & Paulus Y et al. (2010): Restorative retinal photocoagulation. *Invest Ophthalmol Vis Sci* **51**: ARVO e-abstract 5579.
- Maeshima K, Utsugi-Sutoh N, Otani T et al. (2004): Progressive enlargement of scattered photocoagulation scars in diabetic retinopathy. *Retina* **24**: 507–511.
- Mainster MA & Reichel E (2001): Transpupillary thermotherapy for age-related macular degeneration: principles and techniques. *Semin Ophthalmol* **16**: 55–59.
- Mendrinou E, Mangioris G, Papadopoulou DN et al. (2010): Retinal vessel analyzer measurements of the effect of panretinal photocoagulation on the retinal arteriolar diameter in diabetic retinopathy. *Retina* **30**: 555–561.
- Molnar I, Poitry S, Tsacopoulos M, Gilodi N & Leuenberger PM (1985): Effect of laser photocoagulation on oxygenation of retina in miniature pigs. *Invest Ophthalmol Vis Sci* **26**: 1410–1414.
- Muqit MMK, Denniss J, Nourrit V et al. (2011): Spatial and spectral imaging of retinal laser photocoagulation burns. *Invest Ophthalmol Visual Sci* **52**: 994–1002.
- Nagpal M, Marlecha S & Nagpal K (2010): Comparison of laser photocoagulation for diabetic retinopathy using 532-nm standard laser versus multispot pattern scan laser. *Retina* **30**: 452–458.
- Palanker D, Lavinsky D, Blumenkranz MS et al. (2011): The impact of pulse duration and burn grade on size of retinal photocoagulation lesion: implications for pattern density. *Retina* **31**: 1664–1669.
- Paulus YM, Jain A, Gariano RF et al. (2008): Healing of retinal photocoagulation lesions. *Invest Ophthalmol Visual Sci* **49**: 5540–5545.
- Pournaras CJ, Tsacopoulos M, Strommer K, Gilodi N & Leuenberger PM (1990): Scatter photocoagulation restores tissue hypoxia in experimental vasoproliferative microangiopathy. *Ophthalmology* **97**: 1329–1333.
- Sánchez MC, Luna JD, Barcelona PF et al. (2007): Effect of retinal laser photocoagulation on the activity of metalloproteinases and the alpha(2)-macroglobulin proteolytic state in the vitreous of eyes with proliferative diabetic retinopathy. *Exp Eye Res* **85**: 644–650.
- Schatz H, Madeira D, McDonald HR & Johnson RN (1991): Progressive enlargement of laser scars following grid laser photocoagulation for diffuse diabetic macular edema. *Arch Ophthalmol* **109**: 1549–1551.
- Sher A, Leung LS & Leng T et al. (2010): Retinal plasticity and restoration of function after photocoagulation. *Invest Ophthalmol Vis Sci* **51**: e-abstract 2482.
- Spranger J, Hammes HP, Preissner KT et al. (2000): Release of the angiogenesis inhibitor angiostatin in patients with proliferative diabetic retinopathy: association with retinal photocoagulation. *Diabetologia* **43**: 1404–1407.
- Stefánsson E (2006): Ocular oxygenation and the treatment of diabetic retinopathy. *Surv Ophthalmol* **51**: 364–380.
- Stefánsson E, Landers MB III & Wolbarsht ML (1981): increased retinal oxygen supply following pan-retinal photocoagulation and vitrectomy and lensectomy. *Trans Am Ophthalmol Soc* **79**: 307–334.
- Wallow IH (1984): Repair of the pigment epithelial barrier following photocoagulation. *Arch Ophthalmol* **102**: 126–135.

Received on May 15th, 2012.

Accepted on October 27th, 2012.

Correspondence:

Daniel Lavinsky, MD, PhD
Department of Ophthalmology and Hansen
Experimental Physics Laboratory
Stanford University
452 Lomita Mall, room 141
Stanford, California 94305, USA
Tel: + 555182092999
Fax: + 555133302444
Email: daniellavinsky@gmail.com